Supplementary Information for

Narrow-band Polymer Dots with Pronounced Fluorescence Fluctuations for Dual-color Super-resolution Imaging

Zhihe Liu, [‡, a, b] Jie Liu, [‡, a, c] Zhe Zhang,[b] Zezhou Sun,[b] Xuyang Shao,[a] Jintong Guo,[a] Lei Xi,[a] Zhen Yuan,[d] Xuanjun Zhang,[d] Daniel T. Chiu,[e] and Changfeng Wu*[, a]

[a] Department of Biomedical Engineering, Southern University of Science and Technology, Shenzhen, Guangdong 510855, China

[b] State Key Laboratory of Integrated Optoelectronics, College of Electronic Science and Engineering, Jilin University, Changchun, Jilin 130012, China

[c] Department of Biology, Hong Kong Baptist University, Hong Kong, China.

[d] Faculty of Health Science, University of Macau, Taipa, Macau SAR 999078, China

[e] Department of Chemistry, University of Washington, Seattle, Washington 98195, United States.

[‡] These authors contributed equally.

E-mail: wucf@sustech.edu.cn

Experimental Section

Preparation and characterizations of narrow-band BODIPY Pdots. Semiconducting polymer PF5BODIPY565 and PF8BODIPY720 were synthesized as described in previous studies.[1, 2] Narrow-band BODIPY Pdots were prepared by optimizing the nano-reprecipitation method.[3-5] The size distribution of narrow-band BODIPY Pdots was determined by a dynamic light scattering (DLS) instrument (Nano ZSE, Malvern, UK) at 173^{o} back scattering with a 1 cm disposal cuvette. Zeta Potential of narrow-band BODIPY Pdots were measured by DLS in a folded capillary zeta cell (DTS1070). The morphology of narrow-band BODIPY Pdots was investigated on a carbon membrane supported copper grid by a transmission electron microscope (TEM) (HT-7700, Hitachi, Japan) with 100 kV acceleration voltage. Absorption and emission spectra were measured by a UV-vis spectrophotometer (UV2600, Shimadzu, Japan) and fluorescence spectrophotometer (F4600, Hitachi, Japan), respectively. The fluorescent quantum yield was measured by a commercial quantum efficiency measurement system equipped with a semi-integrating sphere fluorescence spectrophotometer with re-excitation correction (QE2100, Otsuka Electronics, Japan).

Bioconjugation and specific subcellular labelling. Streptavidin bioconjugation of narrow-band BODIPY Pdots for single-color subcellular labeling was performed according to our previous reports.[5, 6] We performed dual-color labeling by using PF5BODIPY565-SA to label tyrosinated-α-tubulin (Thermofisher, anti-tyrosinated-α-tubulin, MA1-80017) and PF8BODIPY720-SA to label mitochondrial (Thermofisher, anti-Tom20, PA5-52843). Only one type of biotin-conjugated IgG (Donkey Anti-Rabbit IgG (H+L), 61-82-042418, and Donkey Anti-Rat IgG (H+L), 48-166-040418, Invitrogen) was added each time and then bind to corresponding narrow-band BODIPY Pdots-SA. To avoid cross-labeling between different structures, excessive biotin was used to block the remain binding site of streptavidin-Pdots.

Optical setup. An N-STORM system (Nikon, Japan) configured with a 100× TIRF objective (NA: 1.45) and perfect focus system (PFS) was used to evaluate the photophysical performance of narrow-band BODIPY Pdots and streptavidin conjugated Alexa dyes, including single particle brightness, single particle fluorescent intensity tracking as well as subcellular labeling imaging. An ultrasensitive scientific electron multiplying charge coupled device, EMCCD (Andor, iXon3

Life 897) was used for detecting the fluorescent signal back from the objective. Four laser sources, 405-nm laser (OBIS405LX-100 mW, Coherent, America), 488-nm laser (OBIS488LS-100 mW, Coherent, America), 561-nm laser (Sapphire 561LP-200 mW, Coherent, America) and 642-nm laser (2RU-VFL-P-500-642-B1R, MPB, MPB Communications Inc., Canada) were coupled with an optical fiber and were introduced to an angle adjustable TIRF illuminator. The fluorescence of PF5BODIPY565 and PF8BODIPY720 were filtered by a 562/40-nm single-band bandpass filter (Semrock, FF01-562/40-25) and a 725/40-nm single-band bandpass filter (Semrock, FF01-725/40-25), respectively.

Single-particle imaging of narrow-band BODIPY Pdots and Alexa dyes. For single-particle brightness analysis, 405 nm laser and 561 nm laser were chose for exciting PF5BODIPY565 Pdots and Alexa555, respectively, with the same excitation power density (about 100 W/cm^2) and detection conditions (512×512 pixels with 30 ms exposure time and 50 electron multiplication gain per frame). We chose 405 nm laser and 642 nm laser for excitation of PF8BODIPY720 Pdots and Alexa647 dye with an identical excitation power density (about 100 W/cm^2) and the same detection conditions (30 ms exposure time and 512×512 pixels with 50 electron multiplication gain per frame). Furthermore, for single-particle fluorescence trajectory, 1000 frames were obtained with same excitation light power density (about 100 W/cm^2) and saved as stack images.

Subcellular structures imaging. For imaging of subcellular structures labeled with narrow-band BODIPY Pdots and Alexa dyes, we selected regions of interest (ROI) and changed exposure time to 20 ms, and then set the EMCCD in ‘Frame Transfer’ mode to improve the temporal resolution. The power density of excitation light is well maintained at 100 W/cm^2. For single-color subcellular imaging labeled by narrow-band BODIPY Pdots and Alexa dyes, 1000 frames were captured for SOFI analysis. For dual-color subcellular imaging, 500 frames of PF5BODIPY565 Pdots labeled tyrosinated tubulin and 500 frames of PF8BODIPY720 Pdots labeled Tom20 were captured.

Data analysis methods. Single-particle brightness of narrow-band BODIPY Pdots and Alexa dyes were extracted by running a home-written Matlab code (Mathworks Inc., USA). All single-particle and subcellular sequential images were corrected by running a home-written Matlab

code according to a subpixels drift correction algorithm.[7] Single-particle blinking and off-time interval data were extracted by running a home-written Matlab code. SOFI reconstructed images of single-particle and subcellular cytoskeleton were according to a balanced SOFI algorithm.[8]

Supplementary Figures

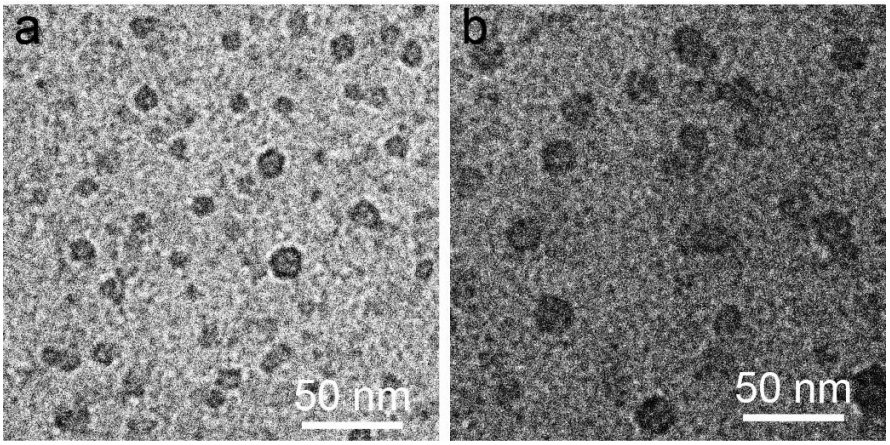

Supplementary Figure S1. Typical transmission electron microscope (TEM) images of (a) PF5BODIPY565 and (b) PF8BODIPY720 Pdots. Scale bar: 50 nm.

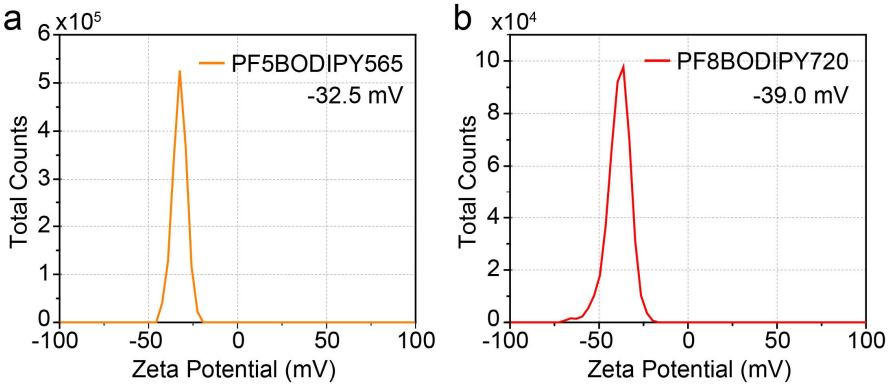

Supplementary Figure S2. Zeta potential of (a) PF5BODIPY565 and (B) PF8BODIPY720 Pdots.

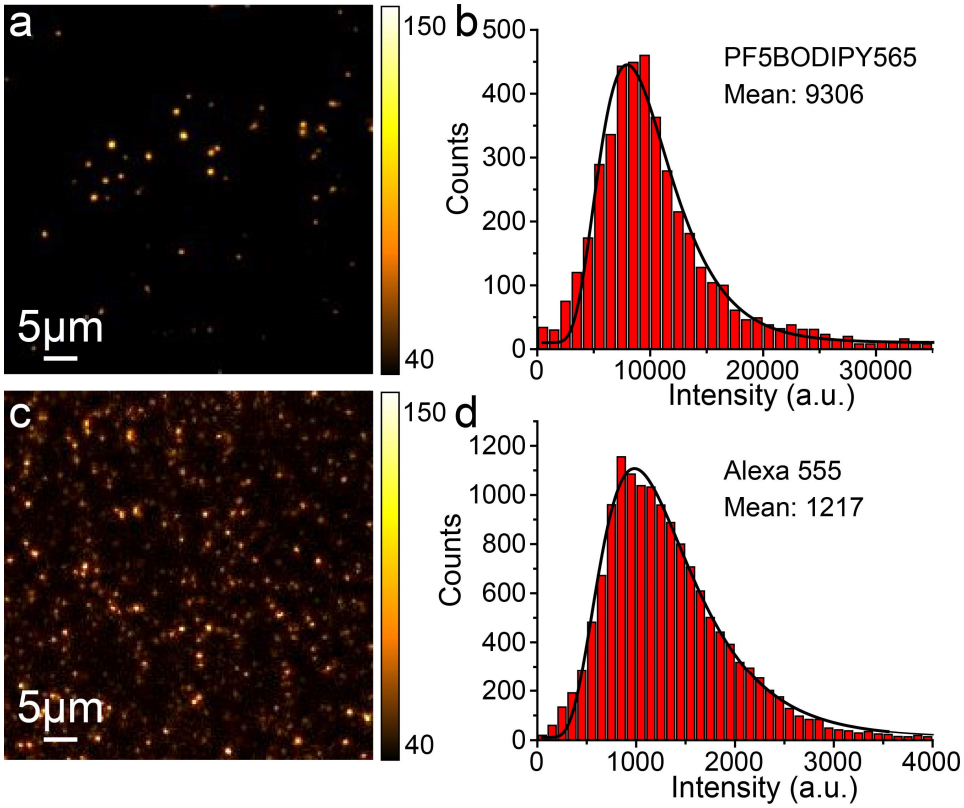

Supplementary Figure S3. Single-particle imaging of PF5BODIPY565 Pdots and Alexa555. (a) and (c) show the single-particle fluorescence images of PF5BODIPY565 Pdots and Alexa555, respectively, obtained under identical excitation light power density and detection conditions. (b) and (d) show the intensity histograms of PF5BODIPY565 Pdots and Alexa555, respectively. The black curves were obtained by fitting a lognormal distribution to the histogram, resulting in average intensities of 9306 and 1217 counts for PF5BODIPY565 Pdots and Alexa555, respectively.

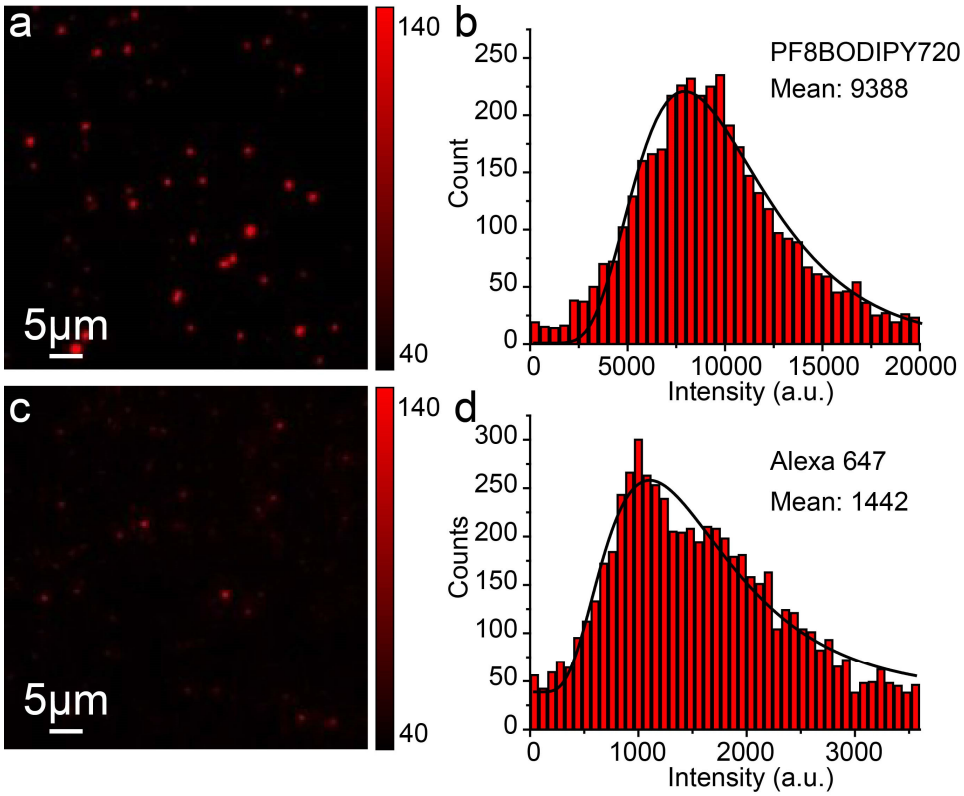

Supplementary Figure S4. Single-particle imaging of PF8BODIPY720 Pdots and Alexa647. (a) and (c) show the single-particle fluorescence images of PF8BODIPY720 Pdots and Alexa647, respectively, obtained under identical excitation light power density and detection conditions. (b) and (d) show the intensity histograms of PF8BODIPY720 Pdots and Alexa647, respectively. The black curves were obtained by fitting a lognormal distribution to the histogram, resulting in average intensities of 9388 and 1442 counts for PF8BODIPY720 Pdots and Alexa647, respectively.

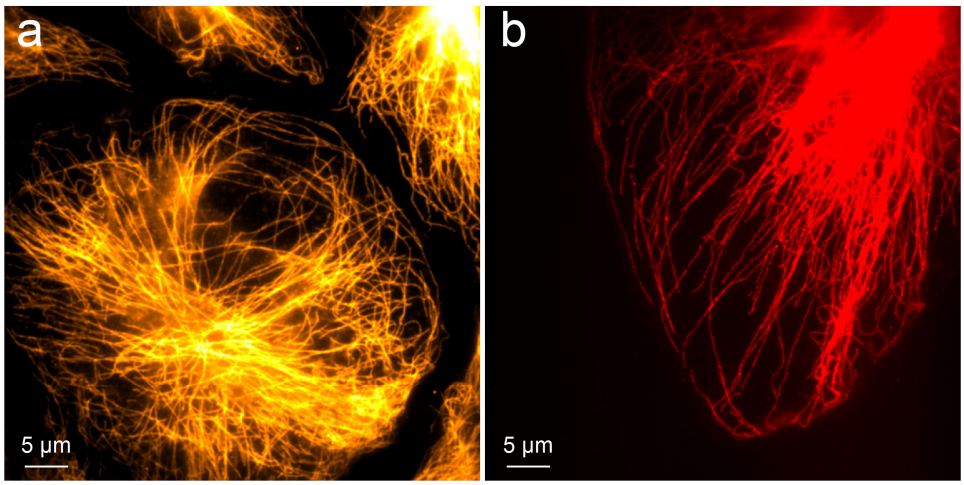

Supplementary Figure S5. Single-color microtubule labeling of (a) PF5BODIPY565 and (b) PF8BODIPY720 Pdots in BS-C-1 cells.

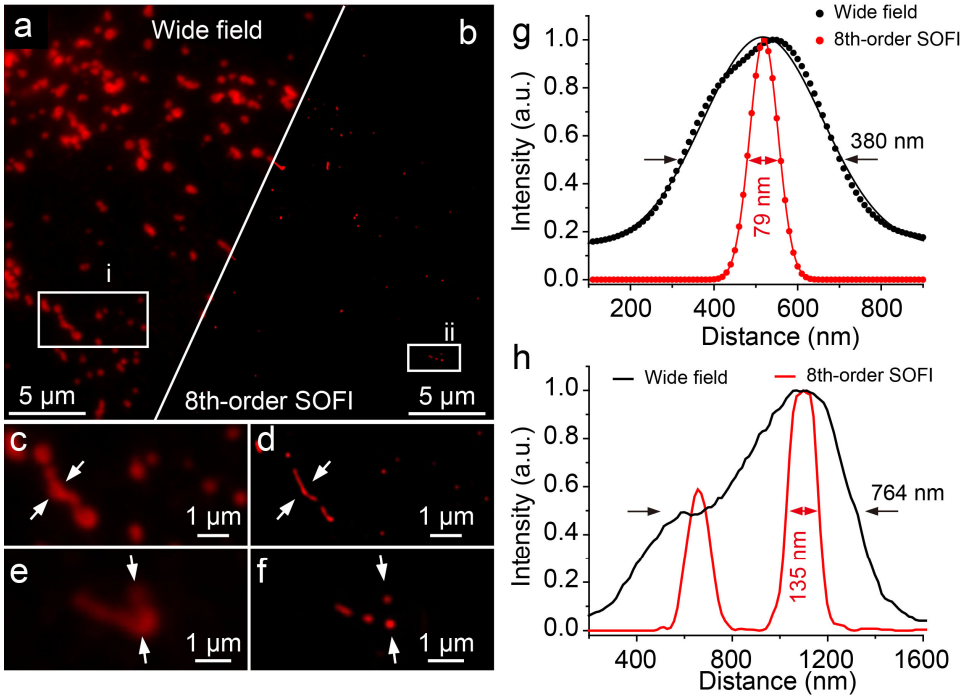

Supplementary Figure S6. Single-color SOFI nanoscopy of PF8BODIPY720 Pdots. (a) Wide-field and (b) the 8th-order SOFI reconstructed images of PF8BODIPY720 labeled mitochondria membrane in BS-C-1 cell. Magnified views of (c) wide-field and (d) the 8th-order SOFI images of section indicated by white box "i" shown in panel a. (e) Intensity profiles of microtubule indicated by white arrows shown in panels c and d. Magnified views of (f) wide-field and (g) the

8^{th}-order SOFI images of section indicated by white box “ii” shown in panel b. (h) Intensity profiles of microtubule indicated by white arrows shown in panels f and g.

Reference:

1. X. Zhang, J. Yu, Y. Rong, F. Ye, D. T. Chiu and K. Uvdal, *Chem. Sci.*, 2013, **4**, 2143-2151.
2. Y. Rong, J. Yu, X. Zhang, W. Sun, F. Ye, I. C. Wu, Y. Zhang, S. Hayden, Y. Zhang, C. Wu and D. T. Chiu, *ACS Macro Lett.*, 2014, **3**, 1051-1054.
3. C. Wu, C. Szymanski and J. Mcneill, *Langmuir*, 2006, **22**, 2956-2960.
4. C. Wu and D. T. Chiu, *Angew. Chem. Int. Ed. Engl.*, 2013, **52**, 3086-3109.
5. X. Chen, R. Li, Z. Liu, K. Sun, Z. Sun, D. Chen, G. Xu, P. Xi, C. Wu and Y. Sun, *Adv. Mater.*, 2017, **29**, 1-7.
6. X. Chen, Z. Liu, R. Li, C. Shan, Z. Zeng, B. Xue, W. Yuan, C. Mo, P. Xi and C. Wu, *ACS Nano*, 2017, **56**, 8084–8091.
7. M. Guizar-Sicairos, S. T. Thurman and J. R. Fienup, *Opt. Lett.*, 2008, **33**, 156-158.
8. S. Geissbuehler, N. L. Bocchio, C. Dellagiacoma, C. Berclaz, M. Leutenegger and T. Lasser, *Opt. Nanoscopy*, 2012, **1**, 1-7.